Available online at www.sciencedirect.com
ScienceDirect
Catalysis Today 119 (2007) 321–326
CATALYSIS TODAY
www.elsevier.com/locate/cattod

Catalytic combustion of toluene over mixed Cu–Mn oxides

M. Zimowska *, A. Michalik-Zym, R. Janik, T. Machej, J. Gurgul, R.P. Socha, J. Podobiński, E.M. Serwicka

Institute of Catalysis and Surface Chemistry, Polish Academy of Sciences, ul. Niezapominajek 8, 30-239 Cracow, Poland

Available online 15 September 2006

Abstract

The influence of the synthesis pH and of the Zn and/or Al additives on the Cu–Mn precursors, obtained by co-precipitation at a constant pH from aqueous solutions of appropriate nitrates at (Cu + Zn)/(Mn + Al) ratio equal 2, was investigated. The relative content of Mn increased with the pH of precipitation. Depending on the sample composition the identified crystalline phases included layered hydroxy double salt, hydrotalcite-like structure, CuO and ZnO. Some precursors had strongly amorphous character. Calcination of the precursors at 673 K resulted in mixed oxides, in which CuO of various degrees of crystallinity could be identified. The Mn-containing phases remained amorphous. All calcined materials proved extremely active in catalytic combustion of toluene. Some catalysts reached 100% conversion already at 403 K. High conversions observed in the low temperature regime were partially due to the strong sorption of toluene. In the catalysts containing Al additive this effect was suppressed.

Keywords: Cu–Mn oxides; Layered precursors; Combustion of toluene; VOCs

1. Introduction

Catalytic combustion is one of the most attractive ways of controlling the emission of volatile organic compounds (VOCs). The advantage of developing the catalysts based on transition metal oxides, rather than on noble metals, is associated with their lower cost, but the possible higher thermal stability and greater resistance to poisoning is also of great importance [1–8]. Both manganese- and copper-based mixed oxide systems serve as efficient catalysts in many industrially important oxidation processes, such as the oxidation of CO, methanol, ethylene, ammonia, nitric oxide and combustion reactions [4–6]. Copper- and manganese-containing catalysts proved also as highly active in the combustion of volatile organic compounds (VOCs) [9–12].

In view of the well known unique properties of mixed oxide phases prepared from the hydrotalcite-like precursors [13,14], our intention was to use such precursors to develop Cu–Mn oxide catalysts for combustion of VOCs.

2. Experimental

A series of Cu–Mn precursors were synthesised by the co-precipitation method at a constant pH, routinely used for the synthesis of layered double hydroxides of the general formula $[M(II)_{1-x}M(III)_x(OH)_2]A_{x/n}^{n-}$. Titration curves of aqueous solutions of $Cu(NO_3)_2{\cdot}3H_2O$ and $Mn(NO_3)_2{\cdot}4H_2O$ used in the synthesis experiments show that upon addition of the NaOH solution the precipitation of hydroxides is complete at pH values of ca. 6 and 9, respectively. In view of the reported observation that the co-precipitation frequently occurs at an intermediate pH value [15], the synthesis of mixed precursors was carried out at pH equal 6, 7, 8 or 9, by dropwise addition of aqueous solutions of $Cu(NO_3)_2{\cdot}3H_2O$ and $Mn(NO_3)_2{\cdot}4H_2O$ to the basic solution of sodium carbonate, using 1 M NaOH for pH control. The obtained precipitates were aged at 328 K for 18 h, then washed and filtered. The final products were dried at 323 K overnight. Following previous reports [11,16–21] it was expected that during synthesis carried out in air Mn(II) would oxidize and provide Mn(III) ions required for the formation of a hydrotalcite structure. In order to provide conditions for precipitation of a hydrotalcite with $x = 0.33$, the Cu:Mn = 2:1 ratio in the nitrate solution was adopted. The resulting solids are referred to as CuMn(x), where x is the synthesis pH value.

* Corresponding author. Tel.: +48 126395191; fax: +48 124251923.
E-mail address: nczimows@cyf-kr.edu.pl (M. Zimowska).

0920-5861/$ – see front matter © 2006 Elsevier B.V. All rights reserved.
doi:10.1016/j.cattod.2006.08.022

Another series of Cu–Mn precursors was synthesised with addition of $Zn(NO_3)_2{\cdot}6H_2O$ and/or $Al(NO_3)_3{\cdot}9H_2O$, in an attempt to induce the formation of the hydrotalcite structures. The overall intended stoichiometry was $\Sigma M(II):\Sigma M(III) = 2:1$, with Cu and Zn entering as M(II), while Mn and Al acting in the capacity of M(III). The following precursors were obtained: Cu:Zn:Mn = 5:1:3, Cu:Mn:Al = 6:2:1, Cu:Zn:Mn:Al = 4:2:2:1. The syntheses were carried out at pH 7, at which the Zn–Al hydrotalcite structure is easily obtained [22], and the samples are referred to as CuZnMn(7), CuMnAl(7) and CuZnMnAl(7). Prior to catalytic tests both series of precursors were heated in air up to 673 K at the rate 10 K/min and annealed at this temperature for 3 h. Catalytic activity of the calcined samples was tested in the reaction of total combustion of toluene in air. The reaction was carried out in a fixed bed flow reactor, in the temperature range of 403–473 K for Cu–Mn(x) catalysts and in the range of 323–573 K for the series of Cu–Mn materials prepared at pH 7 and doped with Zn and/or Al, at toluene concentration 0.2 g/m^3 and GHSV 10,000 h^{-1}. The catalytic activity was measured as ignition curves at increasing temperature (10 K/min). Toluene conversion was calculated by measuring the toluene disappearance by GC-FID (SRI 8610A) and CO_2 evolution by GC-HID (SRI 310). The adsorption–desorption of reactants and products was studied by TPD using a MS detector SRS RGA 200 and the heating rate of 10 K/min.

The synthesised materials were characterized with XRD (Siemens D5005 diffractometer using Cu Kα radiation), XPS (VG-ESCA 3 spectrometer, Al $K\alpha_{1,2}$ radiation, calibration against C 1s from adventitious carbon deposit), BET (N_2 adsorption at 77 K, Quantachrome Autosorb1 Automated Gas Sorption System), and chemical analysis (ICP AES Plasma 40 Perkin-Elmer spectrometer).

3. Results and discussion

3.1. Characterization of the materials

The XRD diagrams of the Cu–Mn precursors show that irrespective of the adopted pH value of the synthesis in no case a hydrotalcite structure has been obtained. However, it is obvious that the pH of co-precipitation influences both the phase composition of the obtained precursors and the amount of the manganese incorporated into the solids (Fig. 1a, Table 1). In the CuMn(6) sample a layered structure of basic copper nitrate $Cu_2(OH)_3NO_3$ is observed. Additionally, the most intense reflections of CuO can be identified. This solid, however, retains only a small amount of Mn used during synthesis (Cu/Mn = 24). Increase of the pH of precipitation results in an increase of the Mn content in the precipitate, but no Mn-containing phase can be detected. The only reflections present in the XRD of the CuMn(7) sample belong to the most intense lines of the layered basic copper nitrate, albeit of lower intensity than in the CuMn(6) material. The CuMn(8) solid is mostly amorphous, the only weak reflections belonging to the layered basic copper nitrate and poorly crystalline CuO. The CuMn(9) sample, whose chemical composition corresponds to the intended one, is completely amorphous.

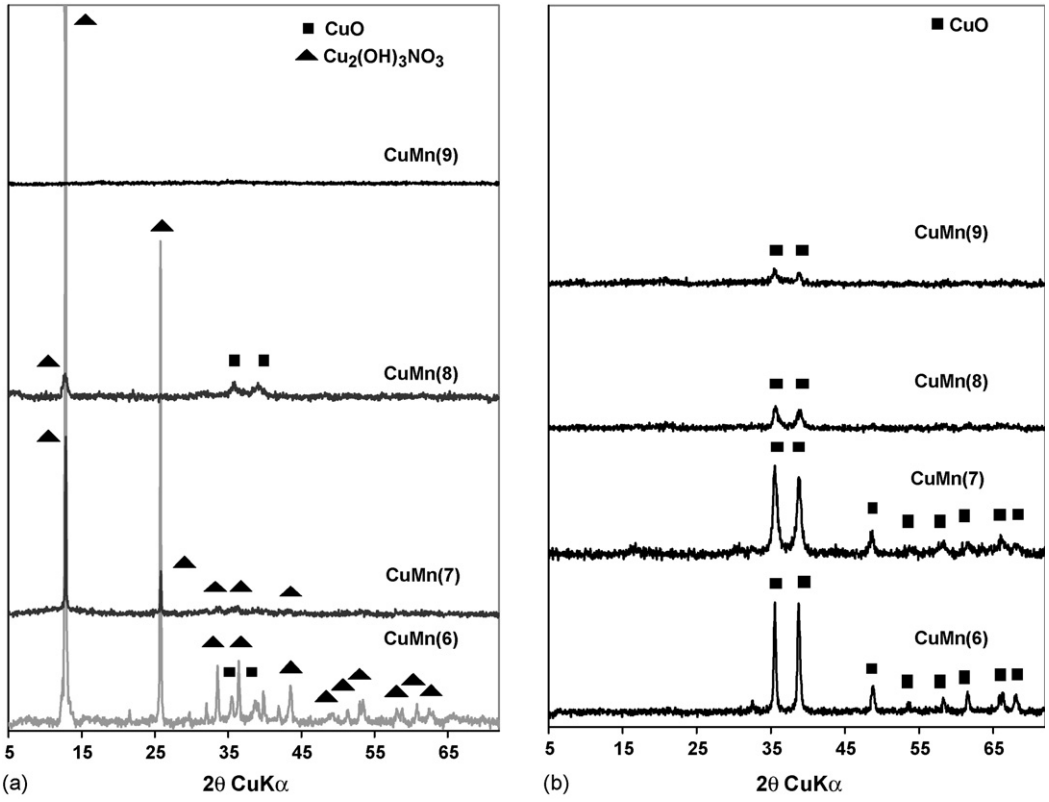

Fig. 1. XRD of CuMn(x) materials: (a) precursors and (b) precursors calcined at 673 K.

Table 1
Chemical analysis of the precursors and the specific surface areas after 3 h calcination at 673 K

Sample	Cu[a]	Mn[a]	Zn[a]	Al[a]	S_{BET} (m^2/g)
CuMn(6)	24.0 (2.0)[b]	1.0	–	–	16
CuMn(7)	3.4 (2.0)	1.0	–	–	60
CuMn(8)	2.3 (2.0)	1.0	–	–	71
CuMn(9)	2.0 (2.0)	1.0	–	–	91
CuZnMn(7)	3.1 (1.7)	1.0	0.7 (0.3)	–	91
CuMnAl(7)	5.1 (3.0)	1.0	–	0.7 (0.5)	97
CuZnMnAl(7)	2.0 (2.0)	1.0	1.4 (1.0)	0.5 (0.5)	109

[a] Atomic ratios with respect to Mn.
[b] Intended values in parentheses.

Replacement of part of copper with zinc in the Cu–Mn system synthesised at pH 7 leads to the appearance in the XRD pattern of CuZnMn(7) of a broad, unidentified reflection in the low range of 2θ (Fig. 2a). Additionally, weak reflections associated with small amounts of layered basic copper nitrate and poorly crystalline zinc oxide can be identified. CuMnAl(7) sample obtained by introduction of aluminium to the Cu–Mn system results in the formation of a hydrotalcite-like structure. In the CuZnMnAl(7) sample, beside the dominant hydrotalcite-like structure, some contribution from the layered basic copper nitrate and zinc oxide is observed.

Chemical analysis shows that the real compositions of the obtained multicomponent solids differ from the theoretical ones (Table 1). The best agreement between the intended and the real composition of the precipitate shows the CuZnMnAl(7) sample.

XRD patterns of the precursors calcined at 673 K for 3 h show only the presence of CuO of different crystallinity and, in the case of Zn-containing samples, traces of ZnO (Figs. 1b and 2b). Analysis of the BET data (Table 1) indicates that the development of the specific surface area of the Cu–Mn mixed oxide phases may be controlled either by increasing pH of synthesis or, for the synthesis carried out at pH 7, by addition of Zn and/or Al.

The surface composition of the calcined CuMn(x) mixed oxides has been characterized by means of the XPS spectroscopy. Analysis of the Cu $2p_{3/2}$ region shows that ca. 70% of surface copper species may be described as Cu^+ (931.3 eV), the rest corresponding to Cu^{2+} (934.3 eV) [23]. The Mn $2p_{3/2}$ spectrum could be decomposed into two major components, with the binding energies of 642.2 eV (ca. 70%) and 640.7 eV (ca. 30%). On the basis of the literature data [23–26] they may

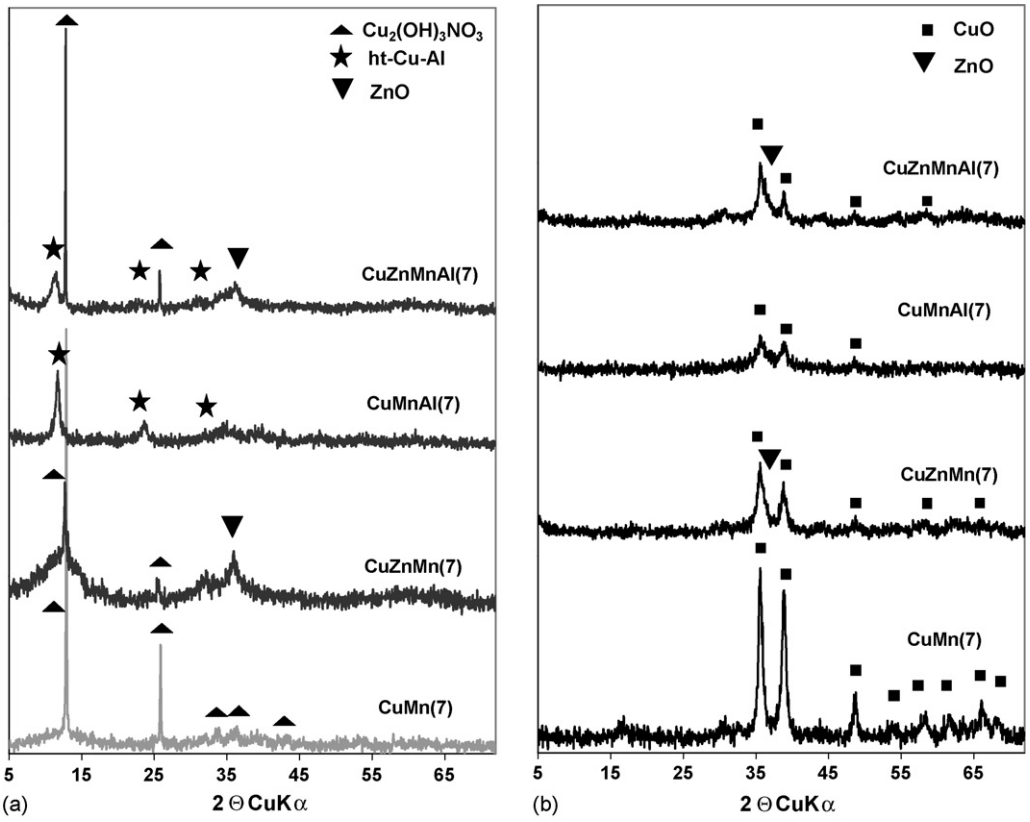

Fig. 2. XRD of CuMn(7) additionally doped with Zn and/or Al: (a) precursors and (b) precursors calcined at 673 K.

Table 2
Surface Cu/Mn ratios (from XPS analysis) and average crystallite size of CuO in CuMn(x) mixed oxides (from XRD by means of the Scherrer equation)

Sample	Cu/Mn	Average crystallite size (nm)
CuMn(6)	1.5 (24.0)[a]	34
CuMn(7)	1.1 (3.4)	12
CuMn(8)	0.9 (2.3)	9
CuMn(9)	0.7 (2.0)	10

[a] Bulk values in parentheses.

be tentatively assigned to Mn^{4+} and Mn^{2+}, respectively. However, the unambiguous determination of the oxidation state of Mn from the binding energies of $2p_{3/2}$ levels may be questioned due to the possible shifts caused by the intra- and/or inter-atomic effects. In the present work the analysis of the Mn 3s splitting, frequently used to distinguish between various oxidation states of Mn [23,27–29], was not conclusive due to the large peak width and partial overlapping with Cu 3p maxima. Therefore, we have analysed the energy difference between the Mn $2p_{3/2}$ and the O 1s levels, whose value depends on the Mn oxidation state [24,30]. For the 642.2 eV maximum the observed energy difference was 112.1 eV, for the 640.7 eV one the difference was 110.8 eV. The results correspond closely to the values reported for Mn^{4+} and Mn^{2+} [24], respectively, and support the assignment based on the $2p_{3/2}$ binding energies. In all cases the surface Cu/Mn ratio is much lower than the bulk value (Table 2), the effect being particularly striking for the CuMn(6) material. The result suggests that the calcined CuMn(x) series may be envisaged as composed of CuO crystallites whose surface is covered with amorphous Mn-rich oxidic coat. The coexistence of Cu^{+} and Mn^{4+}, reported as the most stable configuration in Cu–Mn spinels [23,31,32], may be taken as an indicative of the spinel-like nature of the Mn-containing layer. The exceptionally large difference between the surface and the bulk composition observed in the case of CuMn(6) samples may be understood after analysis of the sizes of CuO crystallites, estimated from XRD data. The CuO crystals present in CuMn(6) sample are much better developed than in other solids. Consequently, the lower surface-to-bulk ratio of the CuO phase diminishes the contribution of copper species in the XPS analysis.

3.2. Catalytic activity

All investigated samples proved extremely active in the reaction of toluene combustion. Fig. 4 shows the toluene ignition curves of the calcined CuMn(x) series. The CuMn(7), CuMn(8) and CuMn(9) samples convert 100% of toluene already at temperature as low as 403 K, while the toluene conversion over the CuMn(6) sample shows an unusual profile, changing from 80% at 403 K to 100% at 473 K with a minimum at intermediate temperatures. The only reaction products are carbon dioxide and water. However, there is a major discrepancy between the amount of apparently converted toluene (Fig. 3a) and the amount of emitted CO_2 (Fig. 3b). At low temperature there is a deficiency of CO_2 with respect to the consumed toluene, while at high

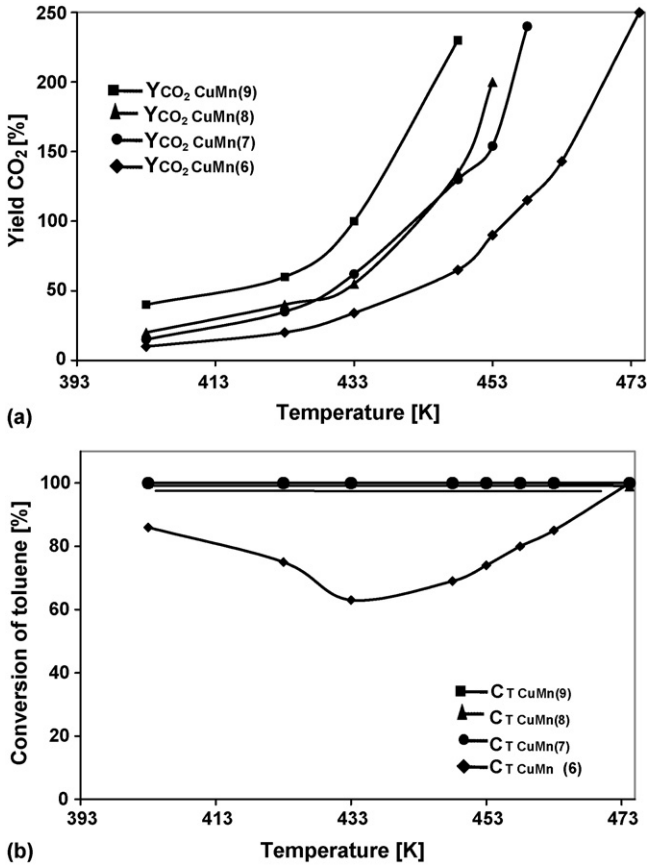

Fig. 3. Catalytic performance of CuMn(x) mixed oxides in combustion of toluene: (a) toluene ignition curves following the toluene signal and (b) toluene ignition curves following the CO_2 signal.

temperature the contrary happens and over 100% CO_2 yield is observed. The phenomenon has been already reported in previous studies on catalytic properties of Mn-based materials in VOCs combustion [9,10,18] and assigned to reactants adsorption/desorption effects. At low temperature toluene is strongly sorbed by the catalysts surface, but only partly catalytically converted to CO_2, which tends to stay at the surface. The high temperature increase of the carbon dioxide yield beyond 100% is due to the combustion of the toluene previously adsorbed at the catalyst surface and desorption of the accumulated CO_2. As the temperature increases both the rate of desorption and the rate of catalytic combustion accelerate, the net effect depending on their relative values. In view of this the initial decrease of toluene conversion on the CuMn(6) catalyst sample may be explained as due to the release of preadsorbed toluene. The effect is not present in the case of other catalysts, because of their higher combustion activity. Indeed, the TPD/MS experiment carried out for the CuMn(6) sample containing toluene preadsorbed at 293 K, confirms that in the case of this catalyst a desorption of toluene precedes its combustion to CO_2 (Fig. 4). Comparison of the CO_2 yield profiles allows for the differentiation between the activities of the catalysts: CuMn(6) $<$ CuMn(7) $\approx$ CuMn(8) $<$ CuMn(9). This shows that the increase of activity is paralleled by the increasing Mn content and the growing specific surface area.

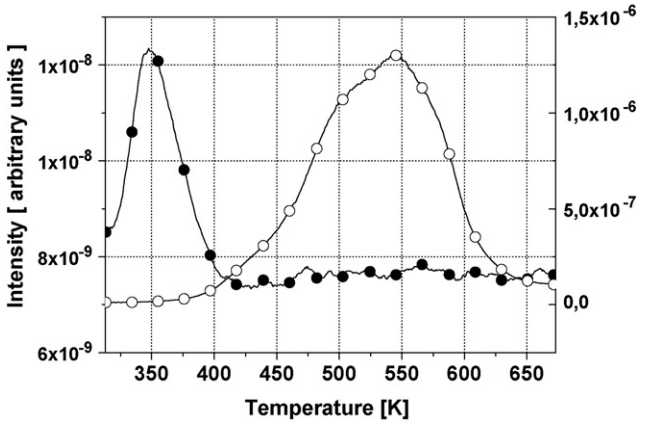

Fig. 4. TPD/MS of CuMn(6) sample containing toluene preadsorbed at 293 K (●, toluene, mass 91; ○, CO_2, mass 44).

Fig. 5a illustrates the influence of Zn and/or Al additives on the catalytic activity of Cu–Mn mixed oxide phases. Although all samples are still very active, it is obvious that the catalysts containing Zn within their composition give poorer performance, while the addition of Al has no such effect. On the other hand, analysis of the CO_2 yield (Fig. 5b) shows that addition of Al lessens the surplus CO_2 formation at higher temperatures, possibly by suppressing the excessive sorption of toluene. This should be considered a beneficial effect, since combustion of toluene is a strongly exothermic reaction and excessive accumulation of toluene on the surface can cause explosion.

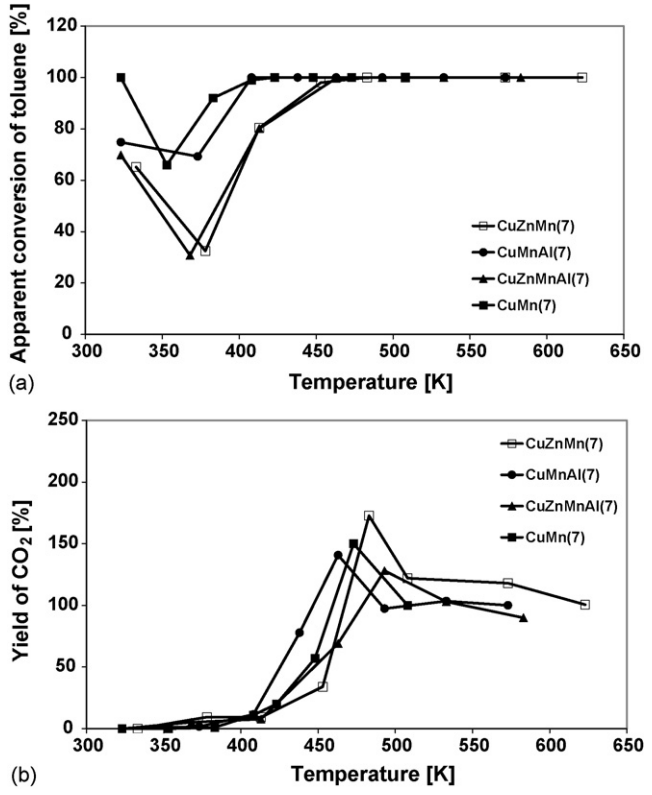

Fig. 5. Influence of Zn and/or Al addition on the catalytic performance of CuMn(7) mixed oxide catalyst in combustion of toluene: (a) toluene ignition curves following the toluene signal and (b) toluene ignition curves following the CO_2.

4. Conclusions

Cu–Mn–O mixed oxides derived from precursors obtained via coprecipitation at a constant pH according to the standard hydrotalcite synthesis procedure are promising catalysts for the total combustion of VOCs. An increase of the manganese amount incorporated into the precursor and related increase of the specific surface area after calcination are favourable for the catalytic activity and may be achieved by an appropriate choice of the pH of the precursor synthesis. The Cu–Mn catalysts may be envisaged as composed of CuO crystallites whose surface is covered with amorphous Mn-rich oxidic coat. All catalysts are extremely active in combustion of toluene. Strong toluene sorption effects are observed in the low temperature regime. Addition of Al is beneficial for the catalytic performance as it suppresses the excessive adsorption of toluene.

Acknowledgement

This work was supported by the Polish Committee for Scientific Research within the research project 3 T08D 003 26 [2004–2006].

References

[1] J.J. Spivey, Ind. Eng. Chem. Res. 26 (1987) 2165.
[2] J. Carpentier, J.F. Lamonier, S. Siffert, et al. Appl. Catal. A: Gen. 234 (2002) 91.
[3] T. Takeguchi, S. Aoyama, J. Ueda, R. Kikuchi, K. Eguchi, Top. Catal. 23 (1–4) (2003) 159.
[4] Y. Liu, M.F. Luo, Z.B. Wei, Q. Xin, P.L. Ying, C. Li, Appl. Catal. B: Environ. 29 (1) (2001) 61.
[5] M. Ferrandon, E. Bjornbom, J. Catal. 200 (1) (2001) 148.
[6] M.C. Alvarez-Galvan, V.A.D.P. O'Shea, J.L.G. Fierro, et al. Catal. Commun. 4 (5) (2003) 223.
[7] H.G. Lintz, K. Wittstock, Catal. Today 29 (1996) 457.
[8] M. Daturi, G. Busca, G. Groppi, P. Forzatti, Appl. Catal. B: Environ. 12 (1997) 325.
[9] S.-W. Baek, J.-R. Kim, S.-K. Ihm, Catal. Today 93–95 (2004) 575.
[10] M. Paulis, L.M. Gand, A. Gil, J. Sambeth, J.A. Odriozola, M. Montes, Appl. Catal. B: Environ. 26 (2000) 37.
[11] S. Velu, N. Shah, T.M. Jyothi, S. Sivasanker, Micropor. Mesopor. Mater. 33 (1999) 61.
[12] W.B. Li, W.B. Chu, M. Zhuang, J. Hua, Catal. Today 93–95 (2004) 205.
[13] A. Vaccari, Catal. Today 41 (1998) 53.
[14] A. Vaccari, Appl. Clay Sci. 14 (1999) 161.
[15] F. Cavani, F. Trifirò, A. Vaccari, Catal. Today 11 (1991) 173.
[16] H.C.B. Hansen, R.M. Taylor, Clay Miner. 26 (1991) 507.
[17] H.C.B. Hansen, R.M. Taylor, Clay Miner. 26 (1991) 311.
[18] R.S. Jayashree, P.V. Kamath, J. Power Sources 107 (2002) 120.
[19] N. Burgos, M. Paulis, A. Gil, L.M. Gandia, M. Montes, Stud. Surf. Sci. Catal. 130 (2000) 593.
[20] T. Grygar, T. Rojka, P. Bezdicka, E. Vecernikova, F. Kovanda, J. Solid State Electrochem. 8 (2004) 252.
[21] F. Kovanda, T. Grygar, V. Dornicak, T. Rojka, P. Bezdicka, K. Jiratova, Appl. Clay Sci. 28 (2005) 121.
[22] F. Kooli, C. Depege, A. Ennaqadi, A. deRoy, J.P. Besse, Clays Clay Miner. 45 (1997) 92.
[23] B. Gillot, S. Buguet, E. Kester, C. Baubet, Ph. Tailhades, Thin Solid Films 357 (1999) 223.
[24] M. Oku, K. Hirokawa, S. Ikeda, J. Electron Spectrosc. Relat. Phenom. 7 (1975) 465.

[25] V. Di Castro, G. Polzonetti, J. Electron Spectrosc. Relat. Phenom. 48 (1989) 117.
[26] J.S. Foord, R.B. Jackman, G.C. Allen, Philos. Mag. A 49 (1984) 657.
[27] C.S. Fadley, D.A. Shirley, Phys. Rev. A 2 (1970) 1109.
[28] I. Barrio, I. Legorburu, M. Montes, M.I. Dominguez, M.A. Centeno, J.A. Odriozola, Catal. Lett. 101 (2005) 151.
[29] V.R. Galakhov, M. Demeter, S. Bartkowski, M. Neumann, N.A. Ovechkina, E.Z. Kurmaev, N.I. Lobachevskaya, Y.M. Mukovskii, J. Mitchell, D.L. Ederer, Phys. Rev. B 65 (2002) 113102.
[30] P. Decorse, G. Caboche, L.C. Dufour, Solid State Ionics 117 (1999) 161.
[31] S. Vepřek, D.L. Cocke, S. Kehl, H.R. Oswald, J. Catal. 100 (1986) 250.
[32] R.E. Vanderberghe, Phys. Stat. Sol. 50 (1978) K85.